electronics

MDPI

Article

IoT-Enabled System for Detection, Monitoring, and Tracking of Nuclear Materials

Carlos A. Hernández-Gutiérrez [1,*], Marcelo Delgado-del-Carpio [2], Lizette A. Zebadúa-Chavarría [3], Héctor R. Hernández-de-León [1], Elias N. Escobar-Gómez [1] and Manuel Quevedo-López [4]

[1] Tecnológico Nacional de México Campus Tuxtla, Carretera Panamericana Km 1080, Tuxtla Gutiérrez C.P. 29050, Mexico
[2] Electrical Department, Universidad Nacional de San Agustín de Arequipa, Santa Catalina No. 117, Arequipa 04001, Peru
[3] Programa de Nanociencias y Nanotecnología, Centro de Investigación y de Estudios Avanzados del Instituto Politécnico Nacional, Av. Instituto Politécnico Nacional 2508, Mexico City C.P. 07360, Mexico
[4] Department of Materials Science and Engineering, University of Texas at Dallas, Richardson, TX 75080, USA; mquevedo@utdallas.edu
* Correspondence: carlos.hg@tuxtla.tecnm.mx

Abstract: A low-cost embedded system for high-energy radiation detection applications was developed for national security proposes, mainly to detect nuclear material and send the detection event to the cloud in real time with tracking capabilities. The proof of concept was built with state-of-the-art electronics such as an adequate Si-based photodetector, a trans-impedance amplifier, an ARM Cortex M4 microcontroller with sufficient ADC capture capabilities, an ESP8266 Internet of Things (IoT) module, an optimized Message Queuing Telemetry Transport (MQTT) protocol, a MySQL data base, and a Python handler program. The system is able to detect alfa particles and send the nuclear detection events to the CloudMQTT servers. Moreover, the detection message records the date and time of the ionization event for the tracking application, and due to a particular MQTT-optimized protocol the message is sent with low latency. Furthermore, the designed system was validated with a standard radiation instrumentation preamplifier 109A system from ORTEC company, and more than one node was demonstrated with an internet connection employing a 20,000 bits/s CloudMQTT plan. Therefore, the design can be escalated to produce a robust big data multisensor network.

Keywords: radiation detection; monitoring network; low latency; IoT applications; MQTT

Citation: Hernández-Gutiérrez, C.A.; Delgado-del-Carpio, M.; Zebadúa-Chavarría, L.A.; Hernández-de-León, H.R.; Escobar-Gómez, E.N.; Quevedo-López, M. IoT-Enabled System for Detection, Monitoring, and Tracking of Nuclear Materials. *Electronics* **2023**, *12*, 3042. https://doi.org/10.3390/electronics12143042

Academic Editor: Domenico Ursino

Received: 18 June 2023
Revised: 9 July 2023
Accepted: 10 July 2023
Published: 11 July 2023

1. Introduction

Nowadays, sensors gather relevant information from the city and citizens, and the communication networks transfer the information in real time. Smart cities are a near-future reality that will improve the quality of life of citizens Ramírez-Moreno et al. [1]. Therefore, the national security of habitants is a critical aspect to focus on. So, nuclear detection systems and security protocols are necessary to protect people from the transportation of nuclear material. The United States has implemented various protocols and measures to enhance the detection of nuclear materials for security purposes. One of the widely used protocols is the National Nuclear Security Administration's (NNSA) Second Line of Defense (SLD) program, which aims to detect and prevent the illicit trafficking of nuclear and radioactive materials [2]. It is essential to mention that both material traffic monitoring and hazard event detection are necessary to improve safety and security. The Internet of Things (IoT) revolution has impacted several areas, such as industrial automatization, health, security, education, and more. The Internet of Things is an emergent technology that refers to a global network of intelligent objects or "things" based on microcontrollers and sensors connected to the cloud. The IoT can improve the current monitoring methods, appropriately supporting the response in real time for various applications, such as those

against COVID-19 [3–7]. However, several issues are still to be overcome, such as the optimization of cloud, edge, and fog computing [8,9]. In addition, network performance, security, compression, and energy management are important considerations for achieving high-performance Internet of Things networks Bedi et al. [10].

That is why high-energy radiation detection is one of the essential tasks conducted by security agencies worldwide to protect their countries from radioactive materials [11,12]. For example, Plutonium (Pu) might be used to construct a nuclear destruction weapon Ruff et al. [13]. Therefore, blind detection from the sea or terrestrial areas means risking vulnerability and the possibility of importing weapons of mass destruction.

On the other hand, it is relevant to mention that there are still issues to overcome in radiation detection, such as the low efficiency in solid-state detectors and false-positive detection due to gamma-ray backgrounds [3]. For example, the detection area of solid-state sensors can be increased to improve the detection efficiency, which, unfortunately, increases the diode leakage current and junction capacitance [14,15]. The density of the leakage current of the photodiode detector should be less than 10^{-10} A/cm^2 to avoid photocurrent reduction during due ionization event. In addition, to avoid a reduction in photosignal, the photodetector density of the capacitance should be less than 1 pF/cm^2. On the other hand, another alternative to detection enhancement is to increase the detectors' density, in which each detector is a pixel within a pixel matrix. For example, a neutron flat array based on photodetectors and thin-film transistors (TFT) was reported by Takeshi Fujiwara et al. [16]. Furthermore, each array of sensors can be connected to the Internet to form an Internet of Things network. A relevant review of the connection between the electronic/photonic array of sensors such as wearables and Internet of Things artificial intelligent was reported by Shi et al. [17]. So, from the literature review, there are reports where the IoT has been used in emergency management systems by utilizing sensor networks and nuclear material detection. The system using the IoT and cloud computing has advantages compared to a GCR system [18–21]. Moreover, the IoT has extra application capabilities, such as target tracking, where many tracking methods and algorithms cover the estimation of the target position and target localization [22]. Specifically, several reports have been published regarding high-energy radiation detection, such as neutron or X-ray. Most of them are related to the neutron monitoring (NM) of cosmic rays. For example, complex embedded systems, including two or three embedded computers such as PIC32, Raspberry Pi, and Arduino, are employed to implement an NM system [23]. Moreover, the connection of NM to the Internet has been carried out through File Transfer Protocol (FTP), which is not an optimized protocol for IoT [24]. B. Wukkadada et al., reported a comparison between HTTP and MQTT in the Internet of Things; they concluded that "MQTT uses less electrical power to maintain an open connection, to receive messages and to send them", so MQTT is a lightweight protocol due to its asymmetric architecture [25]. Regarding the application of IoT for high-energy radiation detection, W. S. Putro et al., reported an updated NM system employing an IoT approach [18]. Saakshi Dhanekar et al., recently reviewed the state of the art of wearable dosimeters and pointed out that IoT can potentially improve radiation detection systems [26]. Unfortunately, they did not demonstrate an experimental IoT radiation detection system in their recent literature review. Daniel Magalotti et al., developed and characterized a personal wireless sensor network for X-ray dosimetry. However, no IoT multi-node was reported even when the TI CC430F6137 RF module was employed for the wireless communication [27]. Vinh Tran-Quang and Hung Dao-Viet reported an Internet of Radiation Sensor System based on the LoRa platform [28]. So, after the literature review [23–32], it is clear that the Internet of Things is key to improving radiation detection and tracking nuclear material. Thus, in this work, an experimental low-cost IoT system is reported and discussed which sends the detected events to the cloud, with the aim of reducing the lack of reports for IoT radiation detection electronic systems. The purpose of this paper is to demonstrate a proof of concept of an IoT system for radiation detection by employing components from the state of the art. Si pin photodetectors, special analog trans-impedance amplifiers able to support high-frequency signals, special

microcontrollers, low-cost IoT modules, and Python-based software to store the detection signal in a MSQL database have been considered, providing valuable elements to operate multisensor networks [33].

2. Materials and Methods

2.1. Sensor and Electronic Readout Design

The sensor and electronic instrumentation, including the microcontroller and the Analog to Digital Converter (ADC) with an interruption capture algorithm, are described below. Later in this manuscript, the IoT module, MQTT protocol, and database have been reported and discussed. The general block diagram of the system is illustrated in Figure 1. From Figure 1, the components such as the detector, circuits, and the different protocols are summarized. The photocurrent response due to alpha particle strikes is provided by a silicon pin photodiode with commercial code OPF480. According to the datasheet, the diode active area is around 0.13 cm^2 with a thickness of 300 μm. The OPF480 device was chosen due to its low leakage current and low capacitance: 0.2 nA and 1.5 pF, respectively, when biased at −5 V. So, its electrical properties are suitable for radiation detection. Afterward, two stages of amplifiers were employed, the first amplifier is a trans-impedance type and the second stage is an inverter amplifier with a filter configuration. The amplification stage is composed of low-noise OPA657 and OPA192 operational amplifiers to perform a gain of about $(500 \times 10^3) \times (5.5) \sim 2.75 \times 10^6$ based on a trans-impedance topology (OPA657). For the trans-impedance amplifier, the photocurrent due to an ionization event flows through to the feedback resistor and generates an output voltage directly proportional to the value of the feedback resistor (10 MΩ for this work). Equation (1) expresses the trans-impedance or current to the voltage converter amplifier.

$$V_{out} = I_{ph} \times R_f \quad (1)$$

where I_{ph} is the photocurrent and R_f is the feedback resistor. The output of the trans-impedance amplifier (V_{out}) is connected in cascade with an inverter filter configuration employing the op-amp (OPA192). A similar transimpedance amplifier was reported by L. O'Brien et al. [34]. The photodetector and the analog amplification stage were set inside a metal box, called a Faraday cage, to isolate the sensor from electromagnetic noise. Figure 2 shows the analog circuitry for signal amplification. In Figure 2, a feedback capacitor is observed in parallel to the feedback resistor of the trans-impedance amplifier. This is a compensation capacitance due to junction capacitance of the photodiode depletion region. The junction capacitance of the photodiode can be modeled as expressed in Equation (2).

$$C_j = \frac{\varepsilon_0 \varepsilon_{Si}}{W} \quad (2)$$

where C_j is the junction capacitance, ε_0 is the permitity in the vacuum (F/cm^2), ε_{Si} is the silicon relative permittivity and W is the extension of the depletion region in (cm^2). Therefore, to achieve the lower capacitance, the depletion region should cover the device completely or be in fully depleted condition. In the case of silicon, a fully depleted condition can be achieved by a highly doped transmitter and a very lightly doped base or active region. Moreover, the active region could be an intrinsic region within a pin photodetector. However, there is a compromise between large depletion region (more than 100 μm) and an incrementation in false positives due gamma-ray interactions, as will be discussed below. From the circuit point of view, the junction capacitance performs a parasitic impedance connected in series with the trans-impedance's feedback resistor, resulting in a frequency filter with RC time constant. This effect is able to perform a filter effect and oscillations in the inverter node. Therefore, to reduce this effect, a compensation capacitor must be connected in parallel with the feedback resistor, reducing the parasitic capacitance and possible oscillations. For this work (0.1 pF), a compensation capacitor was employed according to datasheet recommendations. The impedance of the capacitor

varies inversely proportionally with frequency, achieving short-circuit currents at high frequencies. Therefore, high-frequency noise is not transmitted to the second amplification stage. Since the operational amplifiers are not ideal devices, in a practical situation, the op-amp draws a small current to bias the op-amp at inverting terminal. This bias current results in an error voltage at the output and limits the dynamic range. The situation becomes worse by increasing the feedback resistance because the feedback resistance defines the amplification ratio, and when the current signal is amplified considerably, a small error causes a significant accuracy reduction. Therefore, a low-bias op-amp is critical for practical applications. So, the OPA657 device combines a high gain bandwidth, i.e., high gain-bandwidth product 1.6 GHz, low distortion, high bandwidth 275 MHz (at gain = 10), slew rate 700 V/µs (G = 10, 1-V Step), and a low-voltage noise JFET input stage with a low input bias of 2 pA to offer a very high dynamic range amplifier for high-precision ADC interface.

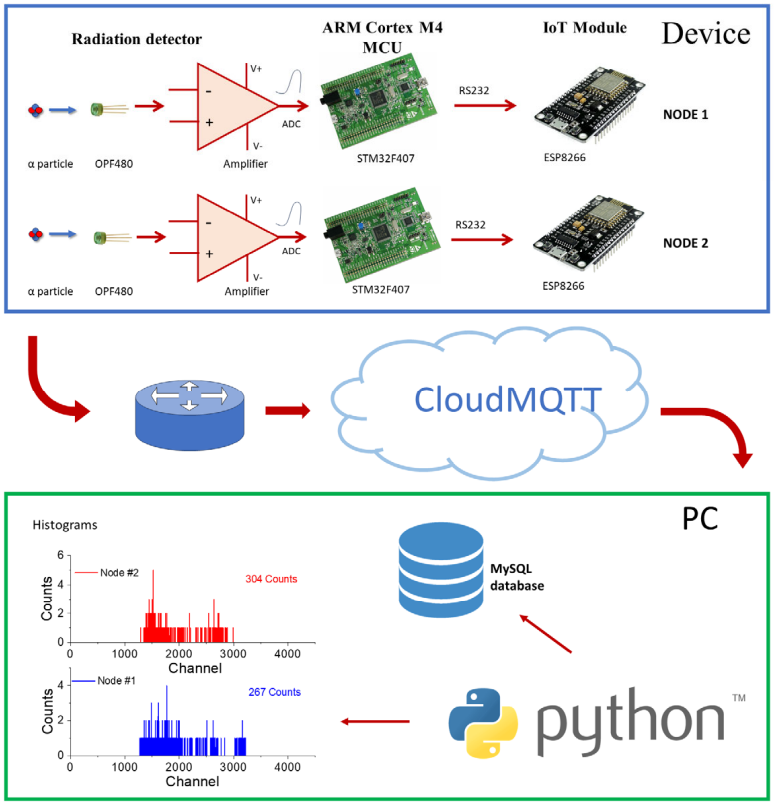

Figure 1. The illustration of the general block diagram of the proposed detection system.

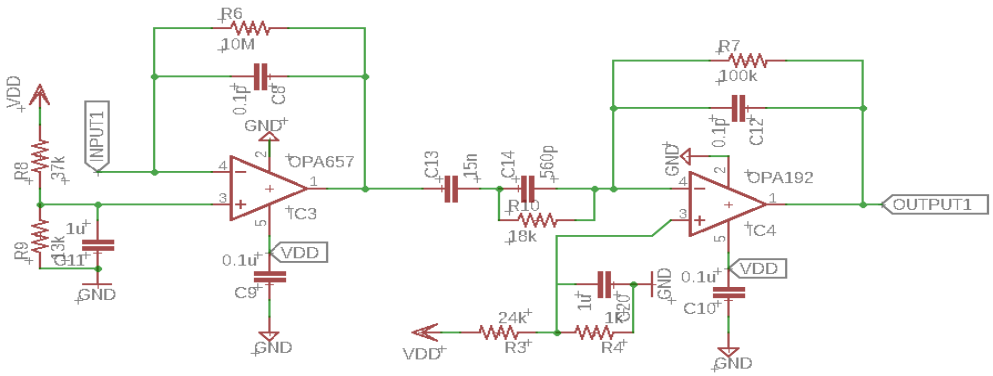

Figure 2. Amplification electronic system. The first stage is the trans-impedance amplifier (OPA657) and the second inverter amplifier stage is based on OPA192.

The STM32F407 microcontroller was chosen to perform the real-time data acquisition to achieve the edge computing stage of the system and send only the necessary data to the cloud. One of the essential characteristics of the ARM Cortex M4 ST microcontrollers is the analog watchdog hardware capability. The integrated ADC allows the readings to be monitored constantly, evaluating if they are within the "guarded area." The guarded area is a voltage range between 0 Volt and a threshold set to 1 Volt. So, an interruption is enabled within guarded area, and released when the ADC readings are out of the guarded area. Therefore, a voltage higher than 1 Volt at the microcontroller PA1 terminal will generate an interruption. The microcontroller was configured to obtain the maximum sample rate from the ADC, such as total conversion time (T_{conv}), calculated as expressed in Equation (3) [29].

$$T_{conv} = \text{Sampling time} + 12 \text{ cycles} \quad (3)$$

According to the datasheet, the minimum sampling time requires 28 cycles, since for lower period values, the interruption caused faults. So, the stable conversion time resulted in 40 cycles. Figure 3 shows the ADC clock configuration details from the datasheet, where T_{conv} in seconds is expressed in Equation (4).

$$T_{conv} = 40 \times (1/36 \text{ MHz}) \quad (4)$$

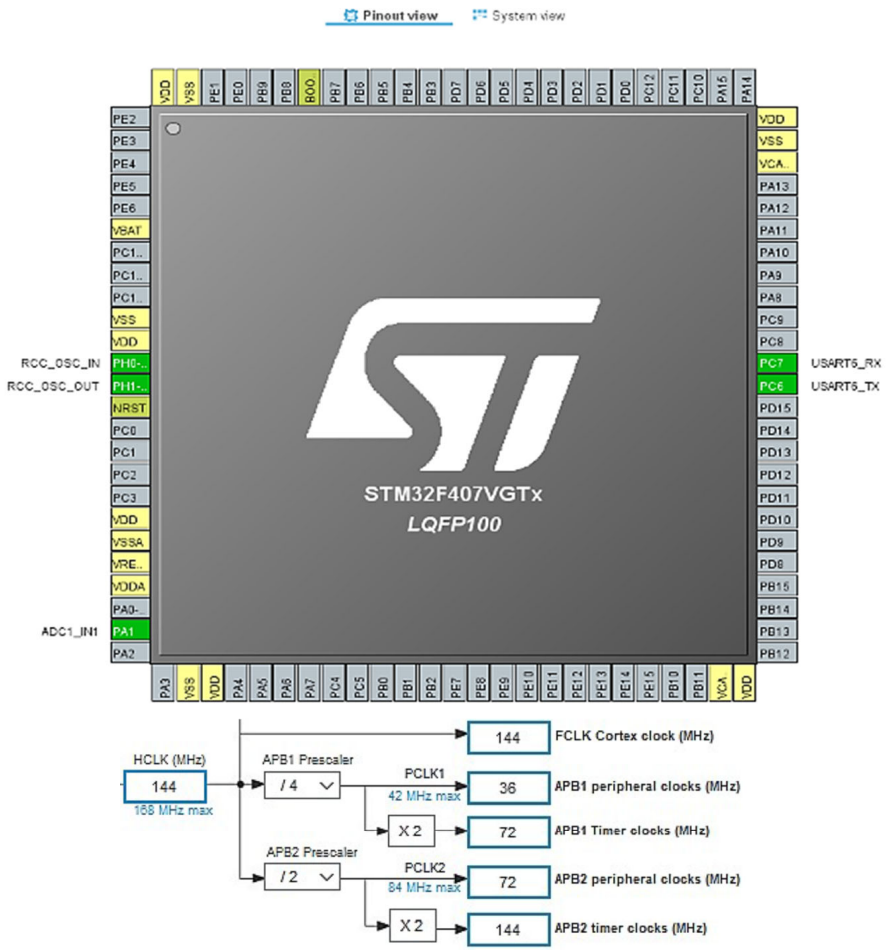

Figure 3. The STM pinout (**top**) and PCLK2 clock configuration (**bottom**) from STMcube32 software and datasheet, respectively.

When the voltage pulse due to a radiation detection event exceeds 1 Volt, the interrupt event occurs, capturing the first sample. Then, due to the voltage at terminal PA1 still being higher than 1 Volt, the microcontroller is interrupted again, obtaining the second and third samples, as illustrated in Figure 4. An algorithm was implemented in the interrupt routine

service (IRS) function to obtain the maximum of the three captured values, reducing the number of data to send according to the edge computing approach. Afterward, the higher obtained value is sent to the IoT module by a Universal Asynchronous Receiver–Transmitter (UART) dedicated hardware configured at 115,200 bits/s. Moreover, an offline validation test employing a serial COM port was conducted to ensure real-time data acquisition. The acquisition algorithm was written in C language employing the Keilkk micro vision development program and is reported below. The amplified signal was obtained by a Tektronix oscilloscope recording program. From Figure 4, it is observed that the amplified signal duration is around 9 microseconds, and the maximum occurs around 3 microseconds. Therefore, our program is able to capture 3 samples to obtain and then send the maximal value of the pulse to the cloud by MQTT protocol as is discussed in the next section.

```
/* Private function prototypes -----------------------------------------------*/
void SystemClock_Config(void);
static void MX_GPIO_Init(void);
static void MX_USART1_UART_Init(void);
static void MX_ADC1_Init(void);
static void MX_TIM3_Init(void);
/* USER CODE BEGIN PFP */

unsigned int value [3];
unsigned int max_value;
volatile unsigned int i = 0;
volatile unsigned int i_sample;
volatile unsigned int i_max = 3;
volatile unsigned int j = 0;

/* Analog Watchdog interrupt service routine */
void HAL_ADC_LevelOutOfWindowCallback(ADC_HandleTypeDef* hadc){
 if(hadc->Instance == ADC1){

        value[i] = HAL_ADC_GetValue(&hadc1);       // Read the ADC
        if(i == i_max){
                i = 0;
                // Find the greatest of 3 numbers
                max_value = value [0];
                for(j=1;j<=i_max;j++){
                        if(value[j]>max_value){
                                max_value = value[j];
                        }
                }
        }else{
                i++;
        }
        HAL_ADC_Start_IT(&hadc1);
}
}

void HAL_UART_RxCpltCallback (UART_HandleTypeDef *huart){
 printf("%c\n\r",buffer);
 HAL_UART_Receive_IT(&huart1,(uint8_t *)&buffer,1);
}
```

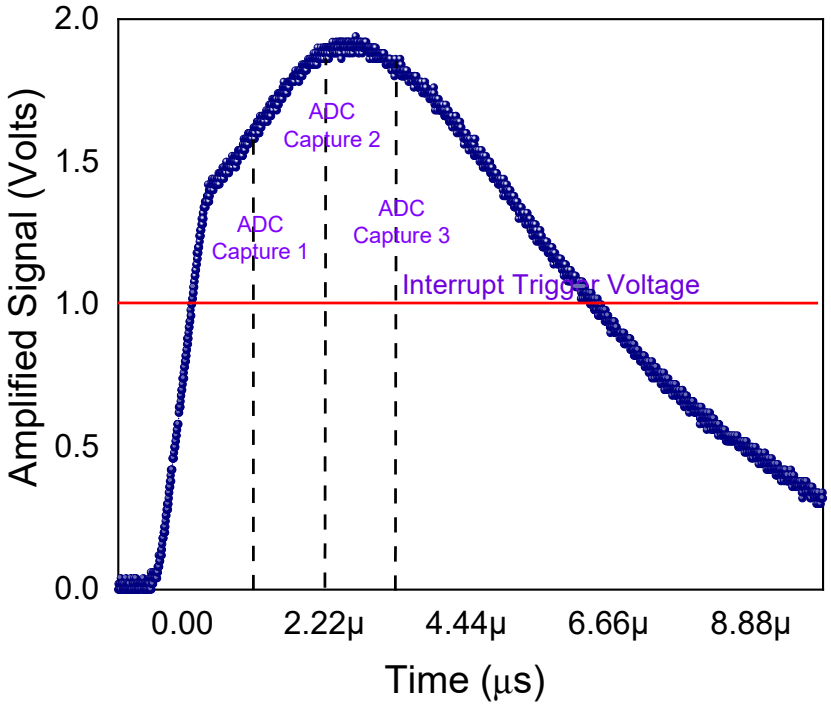

Figure 4. Amplified signal from the incoming current due to alpha ionization event recorded by Tekctronics oscilloscope.

2.2. Internet of Things Module, MQTT, Database, and Processing from the Cloud

After characterization of the electronic system, the acquisition system was evaluated by sending and collecting the data from the cloud. To send data to the cloud, CloudMQTT was employed, which is managed by Mosquitto servers; this service allows us to focus on the application [35,36]. MQTT is an asynchronous communication protocol standardized by the International Organization for Standardization and proposed by IBM in 1999 [37]. MQTT is used for IoT networks due to some unique features, such as being lightweight and capable of handling a communication mode known as publish–subscribe and its reduced payload size compared with the traditional HTTP protocol [38]. A Humble Hedgehog customer plan has been used for our application. In summary, this plan allows 25 connections, 25 users, 25 acl rules, and 3 bridges, which is suitable for sending data at 20 Kbit/s, enough to test our system using two nodes as a proof-of-concept demonstration.

The Python program is responsible for obtaining the data from the CloudMQTT server and storing them in a MySQL database; this is performed by employing the pahomqtt library. MySQL-python library has interacted with the database by executing SQL commands to write and read tables. Since the data are stored in the database, the program reads them and then calculates the counts per channel for each node. Then, the program plots the histograms using the NumPy and matplotlib libraries. Moreover, the counts per channel are saved in two .txt files for documentation and data visualization purposes.

2.3. Proof of Concept of Multi-Nodes, Database, and Processing from the Cloud

For further validation in a real application scenario, detecting two different nodes connected to various networks was performed, emulating two entry ports, N1 and N2, or two sensors connected to a sensor network. An event of 30 s was performed as a test under radiation conditions for each node.

3. Results and Discussion

The photodetector diode was exposed to multiple strikes of alpha particles with energy distributed around 5.2 MeV, employing Polonium 210 as the alpha source. Figure 4 shows the amplified voltage signal due to the current-to-voltage conversion from alpha

detection. Afterward, an ADC integrated into the ARM Cortex M4 microcontroller captured the conditioned signal. The data captured by the ADC were sent to the computer by UART COM and then stored in a Python database program. The radiation test yielded 524 counts over 60 s, corresponding to 8.7 counts/s. The diode and the alpha source were characterized by a standard specialized equipment ORTEC 109A amplifier system to validate the obtained counts under the radiation test [39–41]. The standard ORTEC validation test achieved 615 counts or detections, distributed in a histogram. Figure 5 compares our designed system with the ORTEC commercial system without an Internet connection (offline), whereas Figure 6 shows the data sent to the MQTT servers and then extracted from the cloud. For this test, the proposed system was exposed to 70 s of alpha radiation (online).

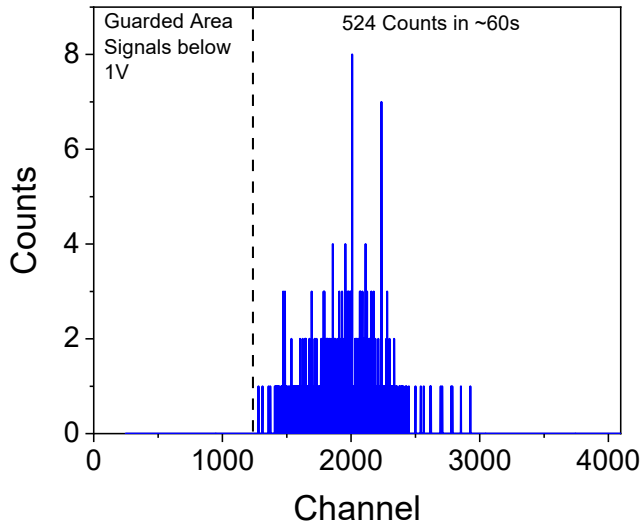

(**a**)

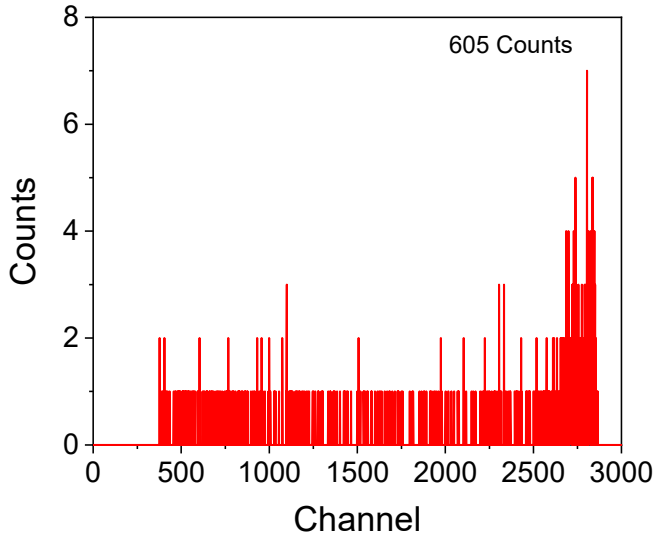

(**b**)

Figure 5. (**a**) Designed system under alpha test for 60 s without internet connection and (**b**) ORTEC system under alpha test for 60 s without internet connection.

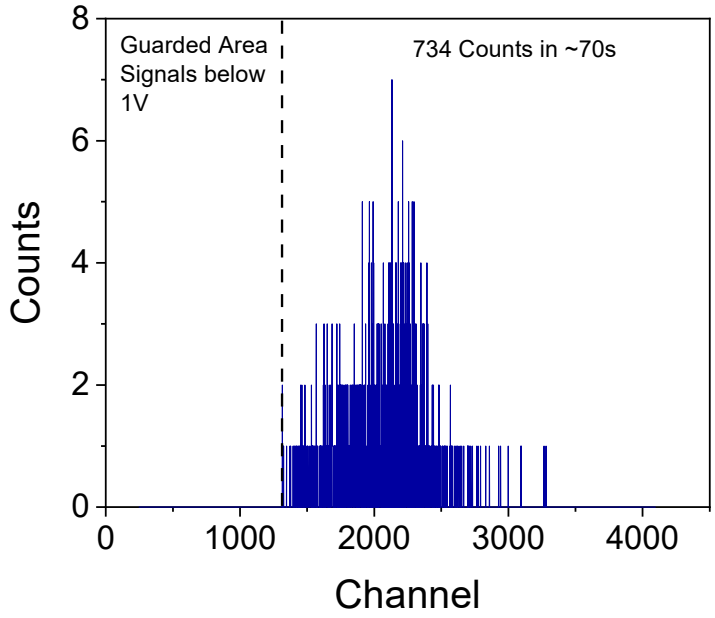

Figure 6. Histogram for the data sent to the cloud broker by MQTT during an exposition of 70 s under alpha radiation.

Figure 7 shows the histograms extracted from the cloud, where 267 and 304 counts were obtained for the nodes N1 and N2, respectively. A slight difference arises from the alpha sources used in each node. The two heads were measured for 1 min in the standard ORTEC system, obtaining 615 counts for the source used in N1 and 901 for the one used in N2. Therefore, the alpha source used in node 2 emits more alpha particles and generates more counts in the detector. Thus, the fewer counts observed on node 1 are due to the difference in the radioactivity of the 210 Polonium sources [42]. Furthermore, it is worth highlighting that our system detects and sends the data to the cloud without losing counts in a very narrow window of only 30 s, which is adequate for a dangerous situation.

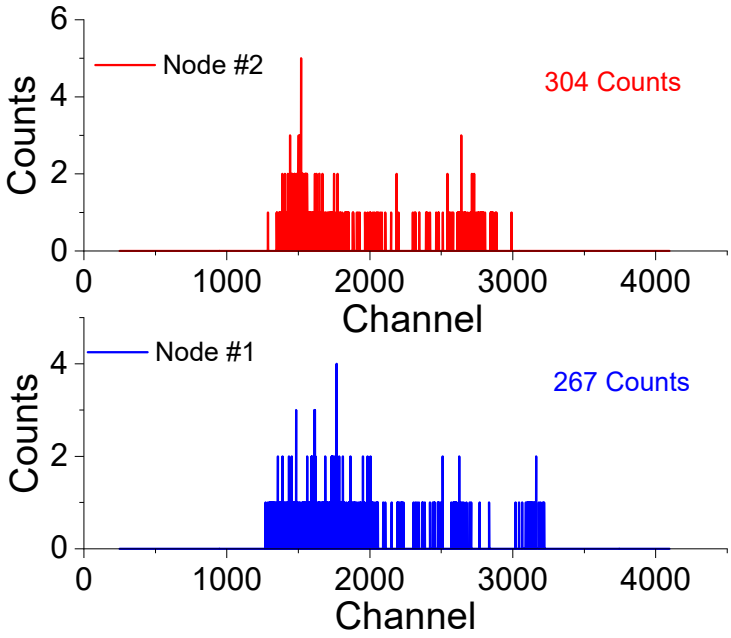

Figure 7. Histogram from the data sent to the cloud broker by MQTT, employing different nodes to emulate a sensor network.

When an ionization event occurs within the photodiode, the amplifier system yields an output voltage of around 1.92 V, corresponding to an incoming photocurrent of ~0.7 μA. The output amplitude depends on the alpha particle scattering with the air medium and can vary due to the distance and angle of incidence. Moreover, the signal's decay time is a function of parasitic capacitance. Therefore, due to the low photodiode capacitance and low input gate JFET capacitance, a short decay time voltage of around 15 μs was observed. Thus, the OPA657 was chosen due to its high bandwidth of 275 MHz and low-input bias current of 2 pA, which can drive a photodiode's capacitance of 49 pF, which is ideal for a trans-impedance amplifier. Furthermore, OPA192 has similar capabilities in comparison with OPA657. The slight difference between our designed system and the ORTEC standard system arises from our policy of eliminating the possible counts below 1 Volt (see Figure 4). The voltage at 1 Volt was chosen after analyzing the amplified signal (Figure 4) because capturing at least three samples over a voltage of 1 Volt is possible. One detection will lie at the maximum voltage peak to send the maximum value to the Internet, reducing the data sent. In contrast, the ORTEC system can count minor variations below channel 500, corresponding to 1.3 Volts corresponding to 12 bits of resolution (11 V/4095 channels). The counts below channel 500 could be associated with noise or false positives, where false positives could be achieved due to the thickness of the photodiode (300 μm) and the gamma-ray background instead of accurate counts. So, our system reduced the possibility of false positives and sent events related to real alpha particles resulting in a detection of almost 9 counts/s. So, the nuclear material could be tracked if the target is moving near the detection nodes. It is essential to remark that the counts with and without the Internet are practically the same as those obtained by the ORTEC system. Therefore, a shallow latency system has been demonstrated due to real-time programming techniques such as analog watchdog interrupt, and the low-latency MQTT protocol is suitable for IoT applications. Furthermore, in Figure 8, it is shown that the system recognized the nodes (N1 or N1), which is also highlighted in the user column of the table, and at the same time recorded the detected peak value and the date and time when the event occurred, allowing tracking and pattern recognition. However, it is important to mention that pattern recognition based on machine learning layer analysis (or any state-of-the-art algorithms) is outside the scope of this work and is a part of future work. Moreover, it is essential to mention that the cloud platform does not allow cloud computing. Therefore, cloud computing services are also outside the scope of this work and are part of future opportunity areas to improve the proposed system. Furthermore, edge computing is performed by a microcontroller with real-time techniques to send only the essential data to the cloud to avoid a compression layer. It is necessary to mention that the present research has shown an alternative for neutron detection for nuclear safety and security systems, prioritizing the possible implementations seizing the advantages of the IoT. IoT-based systems provide elements to configure and implement multisensor networks for location and tracking items [43], and these (multisensor-based tracking systems) are widely enhanced by cloud-based resources [44].

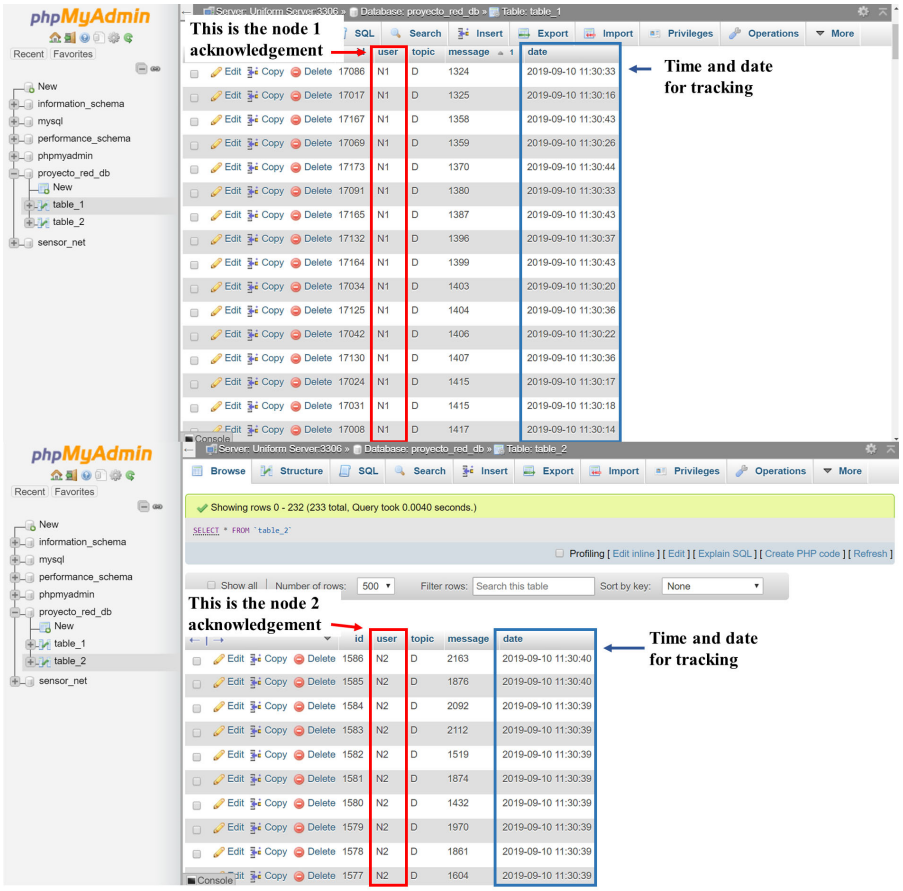

Figure 8. Data collections from the two nodes N1 and N2.

4. Conclusions

In conclusion, we have successfully developed a comprehensive and low-cost IoT-enabled system for alpha particle detection. Our system demonstrates the capability to detect, transmit, and store radiation information in the cloud using the optimized MQTT protocol for the IoT. The performance validation, compared to the standard ORTEC system without an internet connection, revealed practically identical counts per second, confirming the accuracy and effectiveness of our IoT system. Furthermore, our experiments demonstrated the scalability of the system by monitoring two nodes with minimal latency effects. However, it is crucial to expand the data plan bandwidth, which must be incremented as the number of nodes increases to maintain optimal performance. The practical applications of our IoT system are significant, particularly in enhancing security and monitoring radioactive materials. Real-time detection and cloud-based event transmission improve responsiveness and strengthen security measures. Finally, we propose future work to focus on optimizing system performance, exploring advanced algorithms for target tracking, and collaborating with security agencies for real-world evaluations.

Author Contributions: Conceptualization, C.A.H.-G. and M.D.-d.-C.; methodology, M.D.-d.-C., C.A.H.-G. and M.Q.-L.; software, L.A.Z.-C., H.R.H.-d.-L. and L.A.Z.-C.; formal analysis, C.A.H.-G.; investigation, C.A.H.-G.; resources, C.A.H.-G. and M.Q.-L.; data curation, L.A.Z.-C. and M.Q.-L.; writing—original draft preparation, C.A.H.-G.; writing—review and editing, C.A.H.-G. and H.R.H.-d.-L.; visualization, L.A.Z.-C. and E.N.E.-G.; supervision, C.A.H.-G., H.R.H.-d.-L. and E.N.E.-G.; project administration, C.A.H.-G. All authors have read and agreed to the published version of the manuscript.

Funding: This research was supported by TecNM/ITTG, project number 18685.23-P.

Data Availability Statement: The data presented in this study are available on request from the corresponding author.

Acknowledgments: Carlos A. Hernández-Gutiérrez thanks CONACYT Mexico for its international postdoctoral scholarship program and TecNM for project number 18685.23-P.

Conflicts of Interest: The authors declare no conflict of interest.

References

1. Ramírez-Moreno, M.A.; Keshtkar, S.; Padilla-Reyes, D.A.; Ramos-López, E.; García-Martínez, M.; Hernández-Luna, M.C.; Mogro, A.E.; Mahlknecht, J.; Huertas, J.I.; Peimbert-García, R.E.; et al. Sensors for Sustainable Smart Cities: A Review. *Appl. Sci.* **2021**, *11*, 8198. [CrossRef]
2. Cooperative Border Monitoring Opportunities for the Global Partnership. Available online: https://2009-2017.state.gov (accessed on 7 July 2023).
3. Smith, L.; Murphy, J.W.; Kim, J.; Rozhdestvenskyy, S.; Mejia, I.; Park, H.; Allee, D.R.; Quevedo-Lopez, M.; Gnade, B. Thin film CdTe based neutron detectors with high thermal neutron efficiency and gamma rejection for security applications. *Nucl. Instrum. Methods Phys. Res. Sect. A Accel. Spectrometers Detect. Assoc. Equip.* **2016**, *838*, 117–123. [CrossRef]
4. Singh, R.P.; Javaid, M.; Haleem, A.; Suman, R. Internet of things (IoT) applications to fight against COVID-19 pandemic. *Diabetes Metab. Syndr. Clin. Res. Rev.* **2020**, *14*, 521–524. [CrossRef] [PubMed]
5. Rajab, H.; Cinkelr, T. IoT based Smart Cities. In Proceedings of the 2018 International Symposium on Networks, Computers and Communications (ISNCC), Rome, Italy, 19–21 June 2018; pp. 1–4.
6. Zgank, A. Bee Swarm Activity Acoustic Classification for an IoT-Based Farm Service. *Sensors* **2020**, *20*, 21. [CrossRef]
7. Abi Saab, M.T.; Jomaa, I.; Skaf, S.; Fahed, S.; Todorovic, M. Assessment of a Smartphone Application for Real-Time Irrigation Scheduling in Mediterranean Environments. *Water* **2019**, *11*, 252. [CrossRef]
8. Sen, A.A.A.; Yamin, M. Advantages of using fog in IoT applications. *Int. J. Inf. Technol.* **2021**, *13*, 829–837. [CrossRef]
9. Mijuskovic, A.; Chiumento, A.; Bemthuis, R.; Aldea, A.; Havinga, P. Resource Management Techniques for Cloud/Fog and Edge Computing: An Evaluation Framework and Classification. *Sensors* **2021**, *21*, 1832. [CrossRef]
10. Bedi, G.; Venayagamoorthy, G.K.; Singh, R.; Brooks, R.R.; Wang, K.-C. Review of Internet of Things (IoT) in Electric Power and Energy Systems. *IEEE Internet Things J.* **2018**, *5*, 847–870. [CrossRef]
11. Davenport, K. Nations Recommit to Nuclear Security. *Arms Control Today* **2020**, *50*, 34.
12. Nayan, R. The United Nations and Nuclear Issues. *Strategy Anal.* **2020**, *44*, 438–450. [CrossRef]
13. Ruff, T.A. Ending nuclear weapons before they end us: Current challenges and paths to avoiding a public health catastrophe. *J. Public Health Policy* **2022**, *43*, 5–17. [CrossRef]
14. Hernández-Gutiérrez, C.A.; Avila-Avendano, C.; Solís-Cisneros, H.I.; Conde, J.; Sevilla-Camacho, P.Y.; Quevedo-López, M.A. Modeling and SPICE Simulation of the CdS/CdTe Neutron Detectors Integrated with Si-Poly TFTs Amplifiers. *IEEE Trans. Nucl. Sci.* **2022**, *69*, 1310–1315. [CrossRef]
15. Hernández-Gutiérrez, C.A.; Casallas-Moreno, Y.L.; Cardona, D.; Kudriavtsev, Y.; Santana-Rodríguez, G.; Mendoza-Pérez, R.; Contreras-Puente, G.; Mendez-Garcia, V.H.; Gallardo-Hernández, S.; Quevedo-Lopez, M.A.; et al. Characterization of n-GaN/p-GaAs NP heterojunctions. *Superlattices Microstruct.* **2019**, *136*, 106298. [CrossRef]
16. Fujiwara, T.; Miyoshi, H.; Mitsuya, Y.; Yamada, N.L.; Wakabayashi, Y.; Otake, Y.; Hino, M.; Kino, K.; Tanaka, M.; Oshima, N.; et al. Neutron flat-panel detector using In–Ga–Zn–O thin-film transistor. *Rev. Sci. Instrum.* **2022**, *93*, 013304. [CrossRef]
17. Shi, Q.; Dong, B.; He, T.; Sun, Z.; Zhu, J.; Zhang, Z.; Lee, C. Progress in wearable electronics/photonics—Moving toward the era of artificial intelligence and Internetrnet of things. *InfoMat* **2020**, *2*, 1131–1162. [CrossRef]
18. Putro, W.S.; Muztaba, R.; Pratiwi, N.; Putri, A.N.I.; Birastri, W. Internet of Things (IoT) For Galactic Cosmic Ray Application Over Astronomical Observatory in Near Future: A Review Study. *J. Phys. Conf. Ser.* **2019**, *1231*, 12024. [CrossRef]
19. Muhtadan; Abimanyu, A.; Akmalia, R.; Salam, M. Design of IoT-based Radiation Monitor Area for Nuclear and Radiological Emergency Preparedness System in Yogyakarta Nuclear Area. *J. Phys. Conf. Ser.* **2020**, *1428*, 12050. [CrossRef]
20. Krytska, Y.; Skarga-Bandurova, I.; Velykzhanin, A. IoT-based situation awareness support system for real-time emergency management. In Proceedings of the 2017 9th IEEE International Conference on Intelligent Data Acquisition and Advanced Computing Systems: Technology and Applications (IDAACS), Bucharest, Romania, 21–23 September 2017; Volume 2, pp. 955–960.
21. Ji, Z.; Anwen, Q. The application of internet of things(IOT) in emergency management system in China. In Proceedings of the 2010 IEEE International Conference on Technologies for Homeland Security (HST), Waltham, MA, USA, 8–10 November 2010; pp. 139–142.
22. Lu, X.; Liu, J.; Zhao, H. Collaborative target tracking of IoT heterogeneous nodes. *Measurement* **2019**, *147*, 106872. [CrossRef]
23. Strauss, D.T.; Poluianov, S.; Van der Merwe, C.; Krüger, H.; Diedericks, C.; Krüger, H.; Usoskin, I.; Heber, B.; Nndanganeni, R.; Blanco-Ávalos, J.; et al. The mini-neutron monitor: A new approach in neutron monitor design. *J. Sp. Weather Sp. Clim.* **2020**, *10*, 39. [CrossRef]
24. Steigies, C.T.; Thomann, M.; Rother, O.M.; Wimmer-Schweingruber, R.F.; Heber, B. Real-time database for high-resolution Neutron Monitor measurements. In Proceedings of the 30th International Cosmic Ray Conference, Merida, Mexico, 3–11 July 2007; Caballero, R., Medina-Tanco, G., Nellen, L., Eds.; pp. 303–306.

25. Wukkadada, B.; Wankhede, K.; Nambiar, R.; Nair, A. Comparison with HTTP and MQTT In Internet of Things (IoT). In Proceedings of the 2018 International Conference on Inventive Research in Computing Applications (ICIRCA), Coimbatore, India, 11–12 July 2018; pp. 249–253. [CrossRef]
26. Dhanekar, S.; Rangra, K. Wearable Dosimeters for Medical and Defence Applications: A State of the Art Review. *Adv. Mater. Technol.* **2021**, *6*, 2000895. [CrossRef]
27. Magalotti, D.; Placidi, P.; Dionigi, M.; Scorzoni, A.; Servoli, L. Experimental Characterization of a Personal Wireless Sensor Network for the Medical X-ray Dosimetry. *IEEE Trans. Instrum. Meas.* **2016**, *65*, 2002–2011. [CrossRef]
28. Tran-Quang, V.; Dao-Viet, H. An internet of radiation sensor system (IoRSS) to detect radioactive sources out of regulatory control. *Sci. Rep.* **2022**, *12*, 7195. [CrossRef] [PubMed]
29. STMicroelectronics Reference Manual. STM32F405/415, STM32F407/417, STM32F427/437 and STM32F429/439 advanced Arm®-Based 32-bit MCUs. 2021. Available online: https://www.st.com/resource/en/reference_manual/rm0090-stm32f405415-stm32f407417-stm32f427437-and-stm32f429439-advanced-armbased-32bit-mcus-stmicroelectronics.pdf (accessed on 7 July 2023).
30. Russell-Pavier, F.S.; Kaluvan, S.; Megson-Smith, D.; Connor, D.T.; Fearn, S.J.; Connolly, E.L.; Scott, T.B.; Martin, P.G. A highly scalable and autonomous spectroscopic radiation mapping system with resilient IoT detector units for dosimetry, safety, and security. *J. Radiol. Prot.* **2022**, *43*, 011503. [CrossRef] [PubMed]
31. Adumene, S.; Islam, R.; Amin, M.T.; Nitonye, S.; Yazdi, M.; Johnson, K.T. Advances in nuclear power system design and fault-based condition monitoring towards safety of nuclear-powered ships. *Ocean Eng.* **2022**, *251*, 111156. [CrossRef]
32. Sharaf, A.; Zorkany, M.; Shiple, M. High efficient low cost gamma-ray radiation sensor based on IoT platform. *J. Radiat. Res. Appl. Sci.* **2022**, *15*, 100463. [CrossRef]
33. He, S.; Shin, H.; Tsourdos, A. Multi-Sensor Multi-Target Tracking Using Domain Knowledge and Clustering. *IEEE Sens. J.* **2018**, *18*, 8074–8084. [CrossRef]
34. O'Brien, L.; Auer, S.; Gemer, A.; Grün, E.; Horanyi, M.; Juhasz, A.; Kempf, S.; Malaspina, D.; Mocker, A.; Moebius, E.; et al. Development of the nano-dust analyzer (NDA) for detection and compositional analysis of nanometer-size dust particles originating in the inner heliosphere. *Rev. Sci. Instrum.* **2014**, *85*, 035113. [CrossRef]
35. CloudMQTT CloudMQTT Documentation. Available online: https://www.cloudmqtt.com/docs/index.html (accessed on 7 July 2023).
36. Mehmood, M.U.; Ali, W.; Ulasyar, A.; Zad, H.S.; Khattak, A.; Imran, K. A Low Cost Internet of Things (LCIoT) Based System for Monitoring and Control of UPS System using Node-Red, CloudMQTT and IBM Bluemix. In Proceedings of the 2019 International Conference on Electrical, Communication, and Computer Engineering (ICECCE), Swat, Pakistan, 24–25 July 2019; pp. 1–5.
37. Soni, D.; Makwana, A. A survey on mqtt: A protocol of internet of things(IoT). In Proceedings of the International Conference Telecommunication Power Analysis and Computing Techniques, Chennai, India, 6–8 April 2017; pp. 1–5.
38. Yokotani, T.; Sasaki, Y. Comparison with HTTP and MQTT on required network resources for IoT. In Proceedings of the 2016 International Conference on Control, Electronics, Renewable Energy and Communications (ICCEREC), Bandung, Indonesia, 13–15 September 2016; pp. 1–6.
39. Ahmed, K.; Dahal, R.; Weltz, A.; Lu, J.J.-Q.; Danon, Y.; Bhat, I.B. Solid-state neutron detectors based on thickness scalable hexagonal boron nitride. *Appl. Phys. Lett.* **2017**, *110*, 23503. [CrossRef]
40. Kuluöztürk, M.F.; Özgen, S.; Doğru, M. Development of a low noise and low energy consumption alpha spectroscopy amplifier for 222Rn gas detection. *Acta Phys. Pol. A* **2017**, *132*, 789–791. [CrossRef]
41. Huth, G.C.; Trice, J.B.; McKinney, R.A. Internal Pulse Amplification in Silicon p-n Junction Radiation Detection Junctions. *Rev. Sci. Instrum.* **1964**, *35*, 1220–1222. [CrossRef]
42. Carvalho, F.; Fernandes, S.; Fesenko, S.; Holm, E.; Howard, B.; Martin, P.; Phaneuf, M.; Porcelli, D.; Prohl, G.; Twining, J. *The Environmental Behaviour of Polonium*; Technical Reports Series No. 484; International Atomic Energy Agency: Vienna, Austria, 2017; ISBN 9789201121165.
43. Barral, V.; Suárez-Casal, P.; Escudero, C.J.; García-Naya, J.A. Multi-Sensor Accurate Forklift Location and Tracking Simulation in Industrial Indoor Environments. *Electronics* **2019**, *8*, 1152. [CrossRef]
44. Altowaijri, S.; Ayari, M.; El Touati, Y. Impact of Multi-Sensor Technology for Enhancing Global Security in Closed Environments Using Cloud-Based Resources. *J. Sens. Actuator Netw.* **2019**, *8*, 4. [CrossRef]